

Efficacy of Multi-exon Skipping Treatment in Duchenne Muscular Dystrophy Dog Model Neonates

Kenji Rowel Q. Lim,^{1,8} Yusuke Echigoya,^{1,2,8} Tetsuya Nagata,^{3,8} Mutsuki Kuraoka,³ Masanori Kobayashi,⁴ Yoshitsugu Aoki,³ Terence Partridge,^{5,6} Rika Maruyama,¹ Shin'ichi Takeda,³ and Toshifumi Yokota^{1,7}

¹Department of Medical Genetics, Faculty of Medicine and Dentistry, University of Alberta, Edmonton, AB T6G2H7, Canada; ²Laboratory of Biomedical Science, Department of Veterinary Medicine, Nihon University, Fujisawa, Kanagawa 252-0880, Japan; ³Department of Molecular Therapy, National Institute of Neuroscience, National Center of Neurology and Psychiatry, Kodaira, Tokyo 187-8502, Japan; ⁴Department of Reproduction, Nippon Veterinary and Life Science University, Musashino, Tokyo 180-0023, Japan; ⁵Research Center for Genetic Medicine, Children's National Medical Center, Washington, DC 20010, USA; ⁶Department of Integrative Systems Biology, George Washington University School of Medicine, Washington, DC 20010, USA; ⁷Muscular Dystrophy Canada Research Chair, Edmonton, AB T6G2H7, Canada

Duchenne muscular dystrophy (DMD) is caused by mutations in *DMD*, which codes for dystrophin. Because the progressive and irreversible degeneration of muscle occurs from childhood, earlier therapy is required to prevent dystrophic progression. Exon skipping by antisense oligonucleotides called phosphorodiamidate morpholino oligomers (PMOs), which restores the *DMD* reading frame and dystrophin expression, is a promising candidate for use in neonatal patients, yet the potential remains unclear. Here, we investigate the systemic efficacy and safety of early exon skipping in dystrophic dog neonates. Intravenous treatment of canine X-linked muscular dystrophy in Japan dogs with a 4-PMO cocktail resulted in ~3%–27% in-frame exon 6–9 skipping and dystrophin restoration across skeletal muscles up to 14% of healthy levels. Histopathology was ameliorated with the reduction of fibrosis and/or necrosis area and centrally nucleated fibers, significantly in the diaphragm. Treatment induced cardiac multi-exon skipping, though dystrophin rescue was not detected. Functionally, treatment led to significant improvement in the standing test. Toxicity was not observed from blood tests. This is the first study to demonstrate successful multi-exon skipping treatment and significant functional improvement in dystrophic dogs. Early treatment was most beneficial for respiratory muscles, with implications for addressing pulmonary malfunction in patients.

INTRODUCTION

Duchenne muscular dystrophy (DMD) is a lethal X-linked recessive disorder affecting ~1:3,000–1:6,000 boys globally.¹ Symptoms begin at ~3–5 years old, with lower body muscle weakness. This rapidly progresses, leading to body-wide muscle degeneration.^{2,3} Patients are typically wheelchair-bound before their teens, with scoliosis developing after. Cardiorespiratory complications then manifest, often causing death within the third decade of life.^{2,3} In DMD, irreversible pathogenesis occurs before observable phys-

ical signs appear. Newborns with DMD show elevated creatine kinase (CK) levels in blood tests.³ Thus, there is a clear need for DMD patients to receive therapeutic interventions as soon as a diagnosis is reached.

DMD is caused by out-of-frame mutations in the gene for dystrophin (*DMD*), a protein maintaining muscle membrane integrity.^{4–6} Therapies aim to restore dystrophin amounts to functionally beneficial levels in muscle.^{4,7} One approach is exon skipping, which uses short, synthetic antisense oligonucleotides (AOs) to restore the *DMD* reading frame by excluding out-of-frame exons from the final transcript. This strategy is based on the observation that in-frame *DMD* deletions give milder patient phenotypes (Becker muscular dystrophy [BMD]).^{8,9} Exon skipping produces truncated, partially functional dystrophin, which has shown promise in a number of animal studies.^{10–14} Skipping individual exons can treat ~70% of patients with amenable deletions; skipping multiple exons can treat ~90% of this population.¹⁵ Efforts are thus directed at developing multi-exon-skipping cocktails, given their increased applicability.¹⁶

The U.S. Food and Drug Administration (FDA) granted accelerated approval to eteplirsen, a *DMD* exon 51-skipping phosphorodiamidate morpholino oligomer (PMO) by Sarepta, for DMD treatment in 2016.¹⁷ Eteplirsen only rescued <1% dystrophin of

Received 21 June 2018; accepted 16 October 2018;
<https://doi.org/10.1016/j.ymthe.2018.10.011>.

*These authors contributed equally to this work.

Correspondence: Toshifumi Yokota, Department of Medical Genetics, Faculty of Medicine and Dentistry, University of Alberta, Edmonton, AB T6G2H7, Canada.
E-mail: toshifumi@ualberta.ca

Correspondence: Shin'ichi Takeda, Department of Molecular Therapy, National Institute of Neuroscience, National Center of Neurology and Psychiatry, Kodaira, Tokyo 187-8502, Japan.
E-mail: takeda@ncnp.go.jp

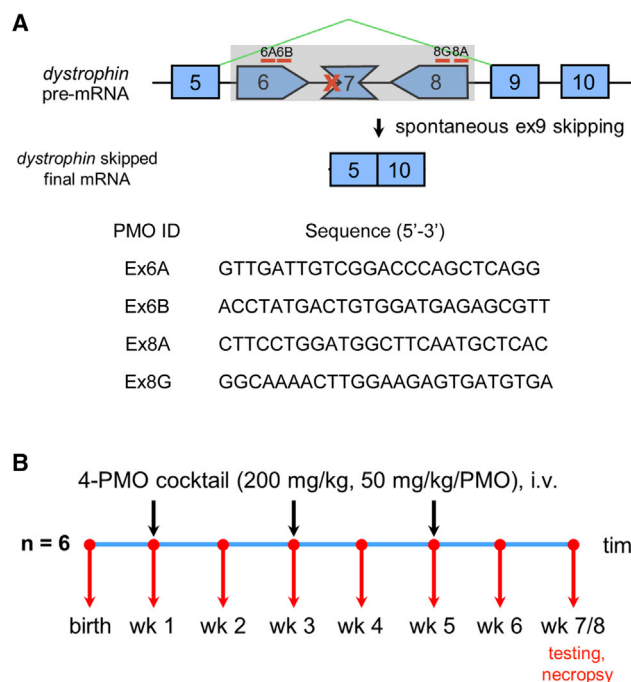


Figure 1. Overview of Experimental Design

(A) Approximate locations of the four PMOs used in the study and the skipped *dystrophin* mRNA after treatment. The sequences of the PMOs are shown below. (B) Treatment schedule for the study; black arrows indicate injection times; red arrows indicate blood collection.

healthy levels after 180 weeks of treatment and did not satisfactorily improve ambulation as of yet.¹⁸ Prior to eteplirsen's approval, the FDA rejected another exon 51-skipping AO—drisapersen (BioMarin)—for reasons of poor safety and efficacy.¹⁹ More recently, results from a trial on another PMO by Sarepta called golodirsen, which skips exon 53, showed a mean dystrophin rescue of ~1% of healthy levels 48 weeks post-treatment.²⁰ Thus, while the efficacy of exon-skipping PMOs in the pre-clinical setting is well established,²¹ their performance in clinical trials can be improved. Given the nature of DMD, early administration of exon-skipping PMOs may improve efficacy. Earlier treatment with corticosteroids and cardioprotective agents (DMD standards of care) better preserved motor and cardiac function, respectively, in patients and dystrophic mice^{22–25}—thus, better outcomes could result from earlier exon skipping.

Here, we tested the efficacy and safety of multi-exon skipping using canine X-linked muscular dystrophy in Japan (CXMD_J) neonates. CXMD_J has a point mutation in the *dystrophin* intron 6 splice acceptor site, which leads to the out-of-frame skipping of exon 7.²⁶ These dogs produce no dystrophin and closely phenocopy DMD patients.²⁷ To rescue the reading frame, at least two exons, 6 and 8, need to be skipped (Figure 1). We previously reported a 3-PMO exon 6–8-skipping cocktail significantly rescuing dystrophin production and remarkably improving muscle function in 2-

5-month-old CXMD_J dogs.¹⁴ Adding another exon-8-skipping PMO further improved efficacy *in vitro*.²⁸ This new cocktail has been tested locally²⁹ but not systemically *in vivo*. Here, we intravenously treated neonatal CXMD_J dogs with this 4-PMO cocktail and analyzed its efficacy, safety, and uptake. Early treatment was non-toxic and induced body-wide exon skipping in skeletal muscles, restoring functional dystrophin levels and improving standing test performance; among muscles, treatment was most beneficial for the diaphragm.

RESULTS

Early Exon-Skipping Treatment Leads to Variable Improvements across Skeletal Muscles

Intravenous treatment of neonatal CXMD_J dogs with the 4-PMO cocktail, consisting of Ex6A, Ex6B, Ex8A, and Ex8G (Figure 1; Table S1), induced body-wide exon skipping in skeletal muscles. The cocktail was administered thrice intravenously every other week, with treatment initiated at 1 week of age. Exon 6–9-skipped transcripts were observed in all examined skeletal muscles by RT-PCR, with skipping efficiencies ranging from ~3%–27% (Figure 2A). Exon 9 was spontaneously skipped due to the nature of *dystrophin* splicing, with the resulting product still in-frame.³⁰ Exon-skipping efficiency was widely variable across muscles, with it significantly increased in the tibialis anterior, gracilis major, and diaphragm compared to non-treated controls, in which little to no exon skipping was observed.

Quantitative analysis by western blotting revealed that early treatment with the 4-PMO cocktail rescued dystrophin synthesis in all analyzed skeletal muscles (Figures 2B and S1). An antibody against the dystrophin rod domain was used (DYS1), ensuring the detection of full-length (Dp427 with exons 6–9 skipped) protein. The extent of dystrophin rescue roughly correlated with the exon skipping efficiency observed in a particular muscle (Figures 2A and 2B). Dystrophin rescue was likewise variable across skeletal muscles. The highest levels of rescue were found in the diaphragm, reaching up to 14% of wild-type levels. The mean rescue in the diaphragm was observably higher in treated compared to non-treated dogs. Dystrophin restoration varied among individual treated dogs, with 10504MA responding particularly well to the treatment and giving the highest amounts of dystrophin rescue observed (Figures 2B and S1). Other dogs showed at most 2% dystrophin of wild-type levels post-treatment. Immunohistochemistry with the same antibody also showed dystrophin protein restoration in all skeletal muscles tested as well as proper sarcolemmal localization (Figure 2C), indicating that the restored dystrophin is potentially functional. Dystrophin-positive fibers were observed in a patched distribution across muscle sections, similar to results from other studies. The number of dystrophin-positive fibers varied across treated dogs, for instance with 8603MA showing a higher abundance of these than others (Figure S2).

The skeletal muscles of treated CXMD_J dogs generally exhibited less degeneration, fibrosis, and necrosis than non-treated

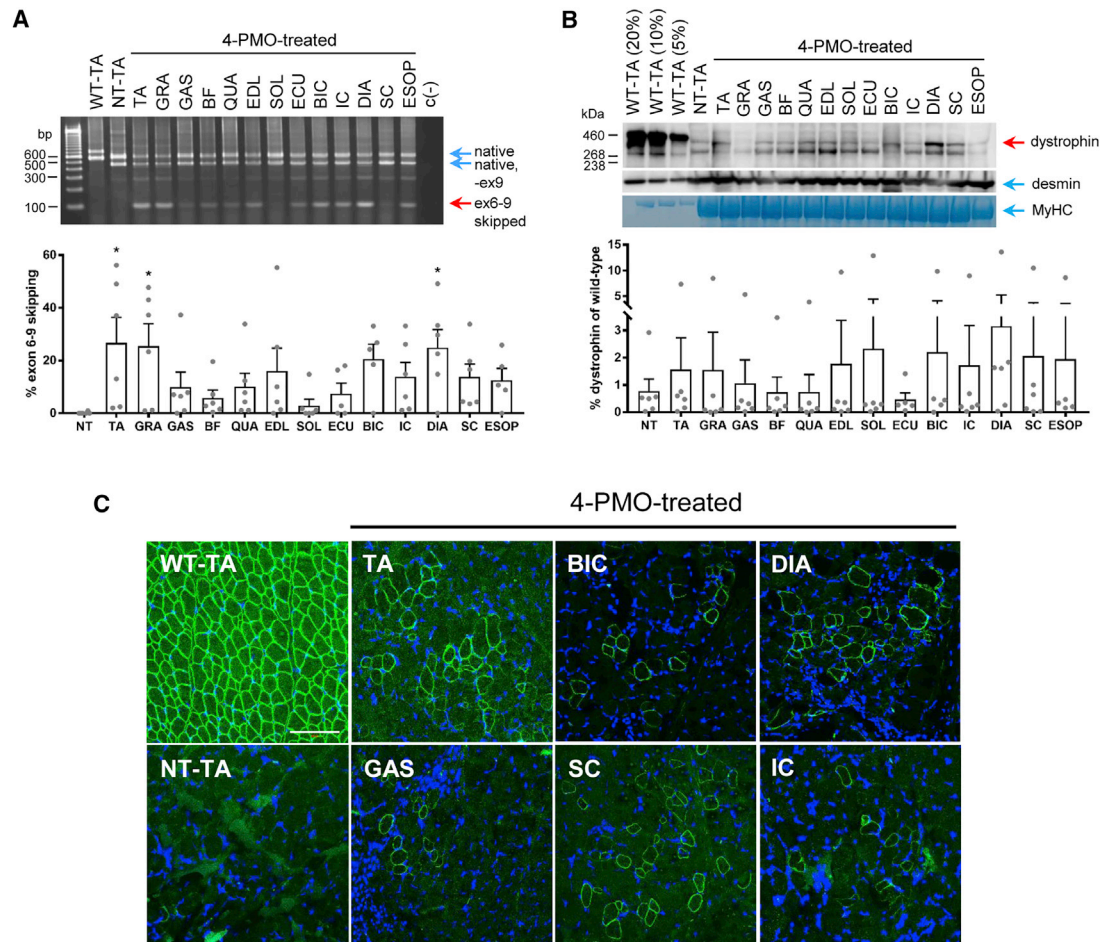


Figure 2. Effects of Early Exon-Skipping Treatment on Dystrophin Production in CXMD_J Skeletal Muscles

(A) Representative RT-PCR image showing exon 6–9-skipped bands across skeletal muscles as a result of treatment with the 4-PMO cocktail. For non-treated (NT) and treated samples, native mutant (exons 5–6–8–9–10) and skipped (exons 5–10) bands are indicated; the rest are intermediate skipping products. Specifically for NT, the band below the native band is due to spontaneous exon 9 skipping. For wild-type (WT), the topmost band is the native (exons 5–6–7–8–9–10) band, while the lower band has exon 9 spontaneously skipped. Calculated exon-skipping efficiencies are shown below. Error bars, SEM; * $p \leq 0.05$ versus NT, one-way ANOVA, Dunnett's multiple comparisons test. Dots represent individual dogs. (B) Representative western blot showing dystrophin rescue in treated CXMD_J skeletal muscles (12303MA). For non-treated and treated muscle samples, 40 μ g of protein was loaded. Dystrophin was detected using DYS1; desmin and myosin heavy chain (MyHC) were detected as loading controls. Dystrophin rescue was quantified relative to 5% WT levels and is shown below. The band observed below the rescued dystrophin band is likely due to the high amount of total protein loaded. Dots represent individual dogs. Error bars, SEM. (C) Representative immunohistochemistry images indicate that the restored dystrophin (green, DYS1) in PMO-treated skeletal muscles localizes correctly to the sarcolemma; blue, nuclei. Total magnification, 200 \times ; scale bar, 100 μ m. For all panels, $n = 5$ –6 (PMO-treated dogs). Abbreviations: TA, tibialis anterior; GRA, gracilis major; GAS, gastrocnemius; BF, biceps femoris; QUA, quadriceps; EDL, extensor digitorum longus; SOL, soleus; ECU, extensor carpi ulnaris; BIC, biceps brachii; IC, intercostal muscles; DIA, diaphragm; SC, sternocleidomastoid; ESOP, esophagus.

dystrophic dogs (Figures 3A and 3B). The fibrotic and/or necrotic area was significantly decreased in the diaphragm of treated dogs (Figure 3B). We also quantified the percentage of CNFs in H&E-stained muscle sections; CNF counts serve as an index of the amount of regeneration that has occurred in a certain muscle. Overall, fewer CNFs were observed in the skeletal muscles of dogs treated with the 4-PMO exon-skipping cocktail (Figure 3C). The reduction in CNF count was significant in the diaphragm and intercostal muscles. This can be because the other skeletal muscles (e.g., tibialis anterior) did not display a dystro-

phic pathology as that in the diaphragm or intercostal muscles of neonatal dogs (Figure 3).

Treatment-Related Dystrophin Rescue Is Not Detectable in Cardiac Muscle Regardless of Early-Age PMO Administration

Early treatment of CXMD_J dogs with the 4-PMO cocktail did not lead to appreciable exon skipping in various cardiac muscles. All examined regions of the heart in treated dogs exhibited exon 6–9 skipping efficiencies of up to 4% (Figure 4A). However, no appreciable increase of dystrophin expression was detected by western blotting with the

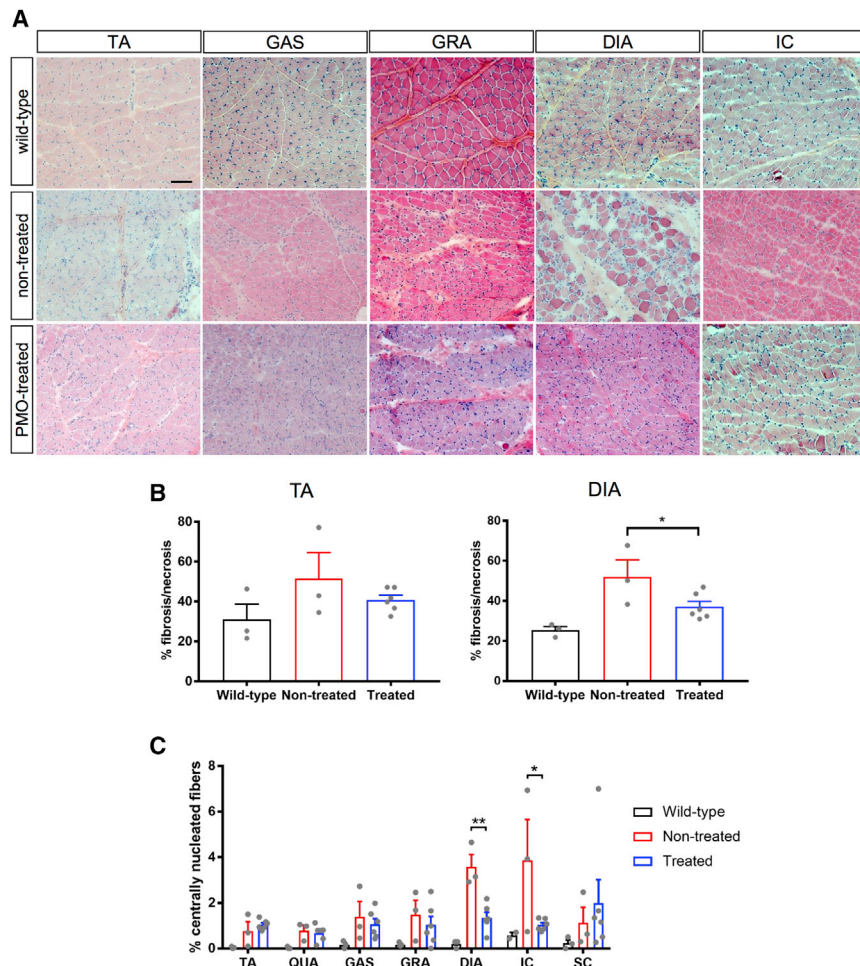


Figure 3. Histopathological Improvements in PMO-Treated Neonatal CXMD_J Skeletal Muscles

(A) Representative H&E-stained sections of various skeletal muscles from PMO-treated CXMD_J dogs, as well as age-matched non-treated CXMD_J and wild-type dogs. Scale bar, 100 μm. (B) Fibrosis and/or necrosis quantification from HE-stained sections of the tibialis anterior (TA) and diaphragm (DIA). n = 3, wild-type and non-treated; n = 6, treated. Error bars, SEM; *p ≤ 0.05, one-tailed Student's t test. (C) Centrally nucleated fiber count quantification from H&E-stained sections of various skeletal muscles. n = 2–3, wild-type; n = 3, non-treated; n = 6, treated. Error bars, SEM; *p ≤ 0.05, **p ≤ 0.01, one-tailed Student's t test. For all plots, dots represent individual dogs. Abbreviations: QUA, quadriceps; GAS, gastrocnemius; GRA, gracilis major; IC, intercostal muscles; SC, sternocleidomastoid.

DYS1 antibody; all cardiac regions examined had around 1% dystrophin of wild-type levels, which non-treated dystrophic cardiac muscle similarly possessed (Figure 4B).

Contrary to expectation, immunohistochemistry with DYS1 showed an absence of dystrophin in the myocardium or Purkinje fiber regions of various cardiac muscles in treated dogs (Figure 4C). Immunostaining with the DYS2 antibody, specific for the C-terminal domain, confirmed the absence of dystrophin isoforms in the myocardium; staining was observed in the Purkinje fiber region, indicating the presence of a non-full-length dystrophin isoform (e.g., Dp71) in these structures, consistent with the previous study of Urasawa et al.³¹ (Figure S3). Thus, the dystrophin protein detected in cardiac muscles via western blotting could either be due to revertant fibers or the presence of putative heart-specific dystrophin isoforms.

PMO Serum Clearance and Muscle Uptake in Treated Neonatal Dystrophic Dogs

ELISA-based detection of PMOs in the sera of treated dogs showed that all four PMOs in the administered cocktail were rapidly

cleared from circulation within a week after an injection; serum samples showed little (generally ≤ 3 nM) to no PMOs between injections as well as during the last weeks of the study (Figure 5A). Noticeably higher concentrations of each PMO were detected in sera collected a day post-injection versus those collected 2 days post-injection, indicative of the short half-life associated with PMOs *in vivo*.

All four PMOs in the systemically administered cocktail had good distribution, with certain levels of accumulation observed in body-wide muscles, including cardiac muscle (Figure 5B).

PMO uptake in muscles was variable across the treated neonatal CXMD_J dogs and across skeletal muscles within individual dogs. Relatively high PMO concentrations were observed in the diaphragm and sternocleidomastoid. Surprisingly, PMO uptake was considerably increased in cardiac muscle across dogs, with PMO concentrations comparable to other skeletal muscles.

In both sera and muscles, strikingly higher concentrations of Ex8G were observed compared to Ex6A, Ex6B, or Ex8A. This is likely due to the tendency of Ex8G to aggregate in solution, despite its low GC content compared to other PMOs in the cocktail. The aggregation of Ex8G may have physiologically increased its retention in the sera and muscles.

Functional Testing of Treated Neonatal CXMD_J Dogs

Four different tests were performed to analyze muscle function in 7- or 8-week-old treated (2 or 3 weeks after the final injection) and non-treated neonatal CXMD_J dogs, as well as in corresponding wild-type controls (Figure 6). Of the functional tests performed, treated neonatal CXMD_J dogs only showed significant improvement in the standing test compared to non-treated controls (Figure 6C).

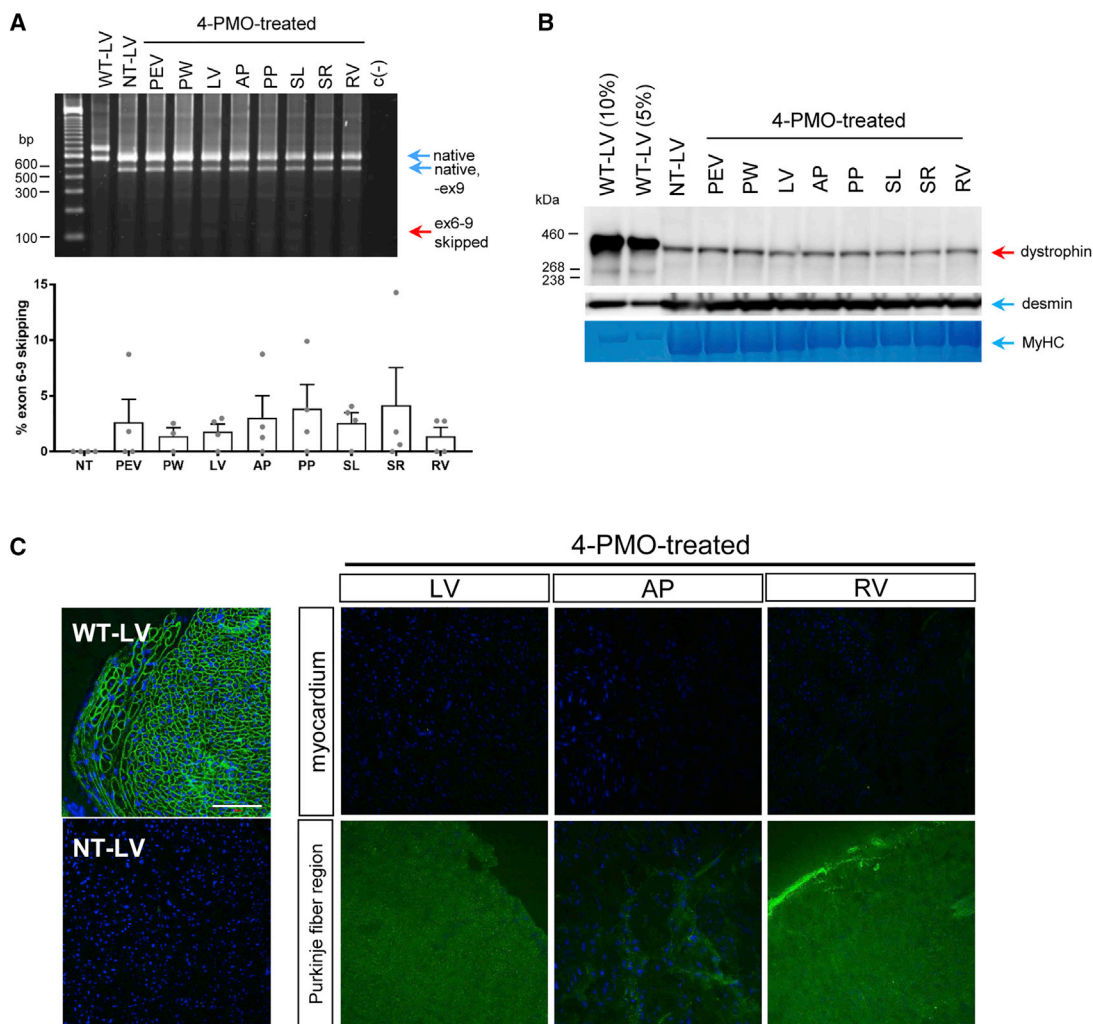


Figure 4. Effects of Early Exon-Skipping Treatment on Dystrophin Production in CXMD_j Cardiac Muscles

(A) Representative RT-PCR image showing exon 6–9 skipping across different regions of the heart after treatment with the 4-PMO cocktail. Native, intermediate, and exon-skipped bands for wild-type (WT), non-treated (NT), and treated samples are indicated as in Figure 2. Exon-skipping efficiencies were quantified, as shown below. Error bars, SEM. Dots represent individual dogs. (B) Representative western blot detecting for dystrophin in various cardiac muscles using DYS1. Desmin and myosin heavy chain (MyHC) were used as loading controls. (C) Representative immunohistochemistry images showing an absence of DYS1 dystrophin signal (green) in treated cardiac muscles, either in the myocardium or the Purkinje fiber region; blue, nuclei. Total magnification, 200 \times ; scale bar, 100 μ m. For all panels, n = 4 (PMO-treated dogs). Abbreviations: PEV, posterior external left ventricle region; PW, posterior wall of the left ventricle; LV, left ventricle; AP, anterior papillary muscle; PP, posterior papillary muscle; SL, left side of the interventricular septum; SR, right side of the interventricular septum; RV, right ventricle.

Early Treatment with Exon-Skipping PMOs Is Not Associated with Detectable Toxicity in Blood Tests

Serum biomarkers for muscle, kidney, liver, and general toxicity were analyzed in weekly blood samples from non-treated and PMO-treated dystrophic neonatal dogs throughout the course of the study. Corresponding wild-type samples were analyzed to provide reference values. CK levels increased with age in both non-treated and treated dystrophic dogs; CK values, however, did not vary widely between the two across all ages. Wild-type CK levels were low at all ages (Figure S4A). Nephrotoxicity was not detected, as blood urea nitrogen (BUN) and serum creatinine

(CRE) levels were similar across all groups, regardless of age (Figure S4B). Hepatotoxicity was also not detectable (Figure S4C). Aspartate aminotransferase (AST) and alanine aminotransferase (ALT) levels, while elevated compared to wild-type values, were similar between non-treated and treated dystrophic dogs in all time points. Gamma-glutamyl transferase (GGT), total bilirubin (TBIL), and serum albumin (ALB) levels did not differ among all groups throughout the study. Levels of other clinical markers (i.e., total protein (TP), lactate dehydrogenase (LDH), alkaline phosphatase (ALP), ion levels) also did not show changes among wild-type, non-treated, and treated dogs (Figure S4D). Based on

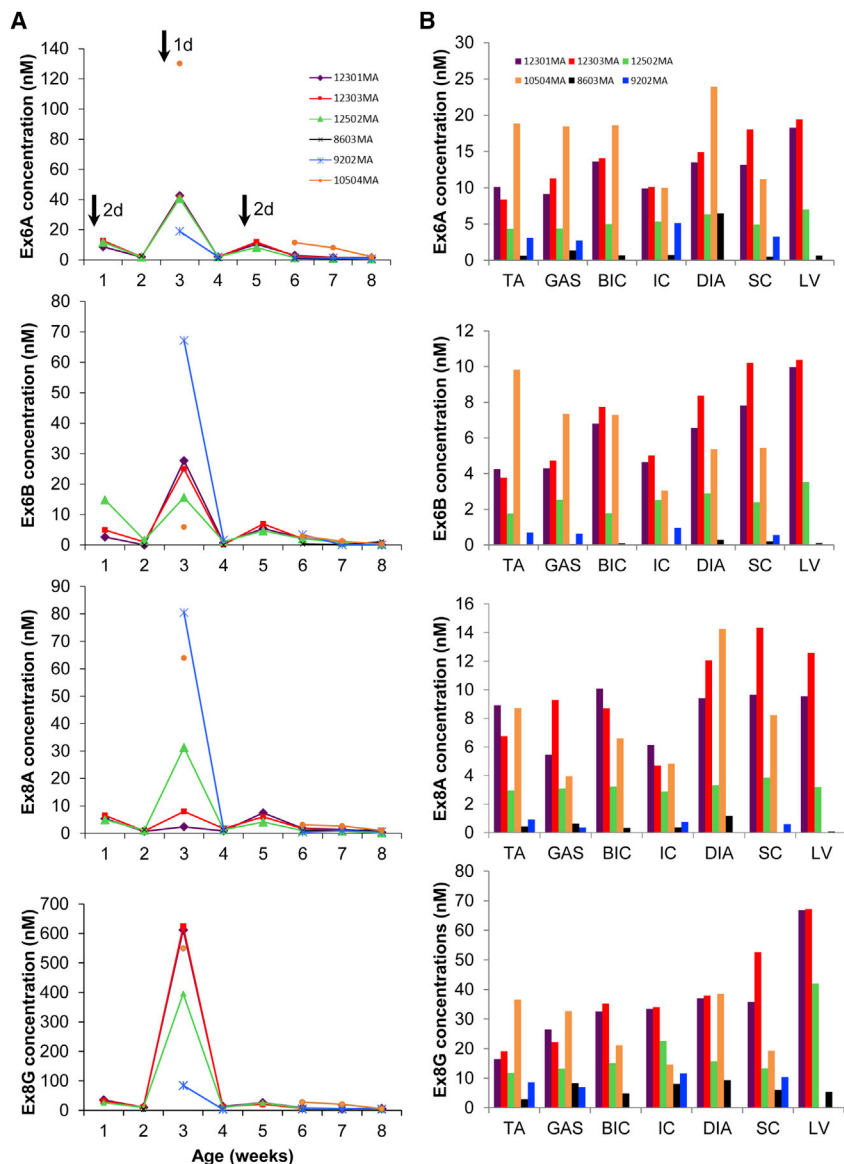


Figure 5. ELISA-Based Quantification of PMOs in Serum and Muscle

(A) Plots show the concentrations of each PMO in the cocktail found in weekly serum samples from treated CXMD_J dogs. Different colors indicate individual dogs. Black arrows in the topmost plot represent times of injection; numbers beside the arrows indicate how many days post-injection sample collection was done. (B) The concentrations of each of the four PMOs in various muscles are shown. Muscles were collected 2–3 weeks after the final injection. Different colors indicate individual dogs. For 10504MA, data for the left ventricle (LV) is not available, while for 9202MA, data for the biceps brachii (BIC), diaphragm (DIA), and LV are not available. For both (A) and (B), n = 4–6 (PMO-treated). Abbreviations: TA, tibialis anterior; GAS, gastrocnemius; IC, intercostal muscles; DIA, diaphragm; SC, sternocleidomastoid.

This is the first demonstration in the neonatal CXMD_J model of the efficacy of early treatment with a multi-exon-skipping PMO cocktail. This is also the first statistically powered investigation of exon-skipping therapy in this model, providing strong insight into the efficacy and safety of exon skipping in a large-animal system.

Early exon-skipping treatment restored dystrophin at varying levels across both muscles and individual dogs; certain muscles only had trace amounts of dystrophin post-treatment (Figures 2B and S1). This variability has been reported in other studies in mice,³³ including our previous study in adult dogs,¹⁴ where some muscles did not respond well to the PMO treatment even at high doses and extended treatments. The factors influencing this are unknown.³³ Skeletal muscle type does not appear to strongly impact exon-skipping outcome; however, the success of PMO delivery into each muscle may have an effect. Interestingly, there

seems to be a disparity between western blotting and immunohistochemistry results (Figures 2B and S2). This might be because the truncated dystrophin with exons 6–9 skipped is less stable than full-length dystrophin and more susceptible to degradation during preparation for western blot. Alternatively, dystrophin rescue along a muscle is typically variable and patchy;³³ it may simply be fortuitous that a high density of dystrophin-positive fibers was observed for 8603MA in the examined sections (Figure S2) than others (Figure 2C).

Early treatment with the 4-PMO cocktail was most beneficial for the diaphragm, which showed the highest levels of dystrophin rescue and the greatest amelioration of histopathology among muscles (Figures 2B and 3). As the diaphragm is one of the first, most severely affected

these, PMO treatment in neonatal CXMD_J dogs did not induce any adverse side effects.

DISCUSSION

The childhood onset of DMD and its progressive nature form a strong rationale for its early treatment. Younger patients are not typically exposed to increased rates of muscular deterioration, presenting better opportunities for preventative treatment. As well, DMD is characterized by the progressive replacement of muscle with fat and connective tissue.³² Exon skipping can only rescue and protect existing muscle fibers, with therapeutic outcome depending on the state of muscle preservation; therefore, earlier treatment provides higher therapeutic value to DMD patients. Here, we sought to determine the advantages, if any, of early exon-skipping treatment *in vivo*.

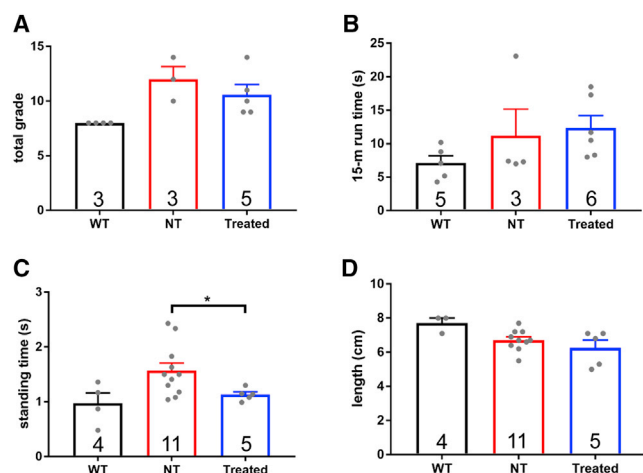


Figure 6. Functional Testing of CXMD_j Dogs

PMO-treated CXMD_j dogs, together with age-matched non-treated (NT) CXMD_j and wild-type (WT) dogs, were subjected to four different functional tests, (A) clinical grading, (B) the 15-m run test, (C) the standing test, and (D) the aperture test. Results for each of these tests are shown. Sample sizes are indicated within the bars. Dots represent individual dogs. Error bars, SEM; * $p < 0.05$, one-tailed Welch t test.

muscles in neonatal dystrophic dogs,³⁴ the finding that it responded well suggests that early exon skipping can oppose the initial stages of muscular deterioration, should it occur (not all skeletal muscles examined in neonatal CXMD_j dogs showed signs of severe degeneration; Figure 3). Further testing will determine if treatment improves respiratory function. Given the central role of the diaphragm in respiration, early treatment with exon-skipping PMOs could be considered for preventing or delaying pulmonary malfunction, one of the leading causes of death in patients.^{3,35}

In adult CXMD_j dogs, intravenous treatment with a 3-PMO cocktail (Ex6A, Ex6B, Ex8A) restored >25% dystrophin of wild-type levels in skeletal muscles such as the triceps brachii and diaphragm; other muscles did not respond as highly.¹⁴ The levels of dystrophin rescue observed here were not as high as those in treated adult dogs—this was likely due to differences in experimental design between the two studies, e.g., treatment frequency and length, and/or due to differences in PMO uptake efficiency or behavior between neonatal and adult dog muscles. Dystrophin restoration accumulates with longer and more frequent exon-skipping treatment.¹³ Potentially higher levels of rescue can be obtained with increased injection frequencies over an extended period of time, as previously reported in the eteplirsen clinical trials.¹⁸ Additionally, this delayed accumulation of dystrophin could explain why the rescue levels observed were not as high as the exon-skipping efficiencies obtained in each muscle. PMOs also have a dose-dependent effect extensively observed in pre-clinical studies; increasing the dose could have been another option. Given these, it is highly encouraging that even with the amounts of dystrophin rescue obtained, treated neonatal dystrophic dogs still showed significant improvements in histology and a test of muscle function, i.e., the standing test. Indeed, this calls into

question what amount of dystrophin rescue can be considered as being “clinically beneficial.” While 10% dystrophin of healthy levels is usually the least amount thought to be of clinical benefit based on BMD patient reference values,³⁶ a study using transgenic mice suggests as low as ~3% of healthy levels can be beneficial.³⁷ Additionally, some amount of therapeutic benefit, though not considerable, was observed with eteplirsen use despite the drug only rescuing <1% dystrophin of normal levels after 180 weeks.¹⁸ The validity of dystrophin as a biomarker for functional improvement will therefore have to be investigated carefully, especially given the many inherent sources of variability associated with its quantification.³³

The mechanisms underlying PMO delivery into dystrophic muscle are an area of active research. It was believed that the compromised permeability of dystrophic muscle was responsible for enhancing PMO entry into tissues.³⁸ Recent evidence, however, suggests that PMO entry is largely influenced by the regenerative or inflammatory state of muscle. Increased PMO uptake was observed in muscle cells undergoing differentiation, as one would observe in actively regenerating muscle, compared to when these cells were proliferating.^{39,40} It was also discovered that macrophages act as PMO reservoirs, taking up large amounts of PMOs and gradually releasing them into their surroundings, increasing the duration these PMOs are available to the muscle.⁴⁰ The clustered, patchy distribution of dystrophin-positive fibers in treated muscle (Figure 2C) supports the above models, as distinct centers of regeneration and inflammation can be found along the length of the dystrophic muscle. Since the majority of skeletal muscles in CXMD_j dogs are not yet in a state of severe dystrophic pathology at an early age (Figure 3), this may have resulted in sub-optimal PMO uptake into tissues. This may be one issue to consider should exon-skipping AOs be administered to young DMD patients. However, early exon-skipping treatment would theoretically be capable of acting on the pathology as soon as it begins, since this provides AOs the opportunity of entry at the earliest signs of muscular degeneration.

The PMO uptake observed in cardiac muscle remains a curious observation (Figure 5B). The levels of cardiac PMO uptake (and even skeletal muscle uptake) we found here were similar to those observed in our previous study in CXMD_j dogs, where we administered peptide-conjugated PMOs (PPMOs) (3-PPMO cocktail, 4 mg/kg/PPMO) instead, a chemistry that exhibits enhanced cardiac uptake.⁴¹ PMOs have historically been known to have poor uptake in the heart,⁴² hence the low-to-nonexistent exon-skipping activity observed. From a previous study of CXMD_j dog hearts, abnormalities, as detected by electrocardiography, echocardiography, and histology, were detectable by 2, 6–7, and 21 months of age, respectively.⁴³ Hence, the increase in uptake cannot be explained by heightened regeneration or inflammation in the heart of neonatal dystrophic dogs. We hypothesize that the conflicting observation of both high PMO uptake and the absence of dystrophin rescue in the heart is due to the increased endosomal trapping of PMOs in cardiac muscle cells. PMOs and most other AOs enter cells via receptor-mediated endocytosis.⁴⁴ Once internalized, AOs must escape from endosomes

to reach their target in the nucleus. AOs have a greater propensity to be trapped in these endosomes in cardiomyocytes than in myotubes *in vitro*.⁴⁵ The conjugation of cell-penetrating peptides to PMOs (i.e., PPMOs) is thought to facilitate endosomal escape, hence the increased activity of PPMOs compared to PMOs.^{46,47} Of course, intracellular mechanisms other than endosomal trapping could have resulted in a similar phenomenon of PMO retention. Thus, in-depth studies of PMO intracellular trafficking in cardiac muscle cells is recommended to better understand PMO uptake in the heart. Findings from these should inform us on how we can better target cardiac muscle with exon-skipping AOs, for instance, by informing a more rational design of cell-penetrating peptides and other AO chemistries.

The present study shows that early treatment with multi-exon-skipping PMOs is safe, as assessed using serum biomarker analysis (Figure S4). There was also no accumulation of the four PMOs in the sera of treated dogs throughout the study (Figure 5A). This implies that early treatment with exon-skipping PMOs should be safe regardless of age, indicating the possibility of applying this strategy to young DMD patients in the clinic. This should also support the inclusion of younger patients in clinical trials for exon-skipping therapies, which would help increase the sample sizes for these trials. On a related note, Sarepta is currently recruiting for a phase II clinical trial that aims to determine the efficacy of eteplirsen treatment in boys with early-stage DMD, aged 4–6 years old.¹⁸ With an estimated completion date of January 2019, results from this trial should shed more light on how useful early exon-skipping treatment is for patients.

In conclusion, early treatment of neonatal CXMD_J dogs with a multi-exon-skipping PMO cocktail led to body-wide exon skipping and dystrophin rescue, as well as the amelioration of dystrophic histopathology, in skeletal muscles with no evidence of toxicity. Early exon-skipping treatment was most beneficial for the diaphragm, with implications for preventing respiratory failure in young DMD patients. The treatment also resulted in some amount of functional improvement. While the efficacy in cardiac muscles was low, there was a surprisingly high uptake of PMOs in the dog heart, an observation that warrants further investigation. A more extended study is recommended to determine the efficacy of early exon-skipping treatment in the long run. Though not many, a certain population of patients with point, duplication, and deletion mutations amenable to exon 6 and 8 skipping have been enrolled in DMD mutation databases (Universal Mutation Database – Duchenne muscular dystrophy [UMD-DMD] and Leiden Open Variation Database [LOVD]). We have previously demonstrated *in vitro* translation of the 4-PMO cocktail for the dog model to a patient with an exon 7 deletion.²⁸ The *in vivo* finding shown here further confirms the therapeutic potential of exon 6 and 8 skipping to such patients. Finally, as the technology for facilitating DMD diagnosis continues to advance, safe and effective therapies can be provided at an earlier time to patients. This enables us to act on the disease before it even manifests, potentially generating more improved health outcomes for patients with DMD.

MATERIALS AND METHODS

Animals

Animals were housed at the National Center for Neurology and Psychiatry (NCNP) in Tokyo, Japan following guidelines by their Ethics Committee for the Treatment of Laboratory Middle-Sized Animals. All procedures were reviewed and approved by the respective Institutional Animal Experiment Committees at NCNP. A listing of animals used, with information on respective experimental groups and the procedures conducted for each, is provided in Table S1. Genotyping confirmed the presence of the CXMD_J mutation.

Intravenous PMO Treatment and Sample Collection

PMO sequences and target regions are in Figure 1A; sequences were based on our previous work.^{14,28} A cocktail consisting of Ex6A, Ex6B, Ex8A, and Ex8G, each synthesized by Gene Tools, was prepared in saline with 50 mg/kg/PMO (total 200 mg/kg). Intravenous injection of the cocktail into CXMD_J dogs via the saphenous vein was performed as described.⁴⁸ Injections were done every other week, at 1, 3, and 5 weeks of age (Figure 1B). Weekly blood samples were collected for toxicity testing. At 2–3 weeks after the final injection, dogs were subjected to functional testing and then euthanized by exsanguination while under general anesthesia. Muscle samples were collected as previously described.⁴⁹ Corresponding muscles were also collected from age-matched non-treated CXMD_J and wild-type dogs.

Functional Assessment

Four functional tests were done: clinical grading, 15-m run, standing, and maximum open-mouth width determination. Clinical grading was done as previously described⁵⁰ to assess overall condition or phenotype using standardized five-point scales. In the 15-m run test, the time it took to traverse a 15-m distance was recorded. For the standing test, dogs were laid in a lateral recumbent position and the time for each dog to stand back up was recorded. The 15-m run and standing tests were repeated up to five times per dog; the average across all trials was obtained. Finally, the maximum open-mouth distance for each dog was measured to evaluate jaw joint contracture. All tests were performed by handlers (led by, and including, M. Kuraoka) blinded to the treatment allocation.

Exon-Skipping Efficiency Determination

Exon-skipping efficiencies were determined as previously described,⁴⁹ with modifications below. cDNA was synthesized from 1,000 ng of total RNA using SuperScript IV reverse transcriptase (Invitrogen), with 2.5- μ M random hexamers (Invitrogen) and a final volume of 20 μ L; a reaction containing nuclease-free water instead of RNA served as a negative control. PCR was performed with 8 μ L of cDNA or negative control using GoTaq (Promega). To detect skipping, a forward exon 5 primer (5'-CTGACTCTTGTTTGATTTGGA-3') and a reverse exon 10 primer (5'-TGCTTCGGTCTCTGTCAATG-3') were used at final concentrations of 0.3 μ M. The following program was used: (1) 95°C, 2 min; (2) 40 cycles of 95°C, 30 s; 60°C, 30 s; 72°C, 42 s; (3) 72°C, 5 min; (4) 4°C, hold. PCR products were run on an agarose gel, and band intensities were

quantified using ImageJ (NIH). Exon skipping efficiency was calculated using $([\text{skipped band intensity}]/[\text{total intensity of native, intermediate, and skipped bands}]) \times 100 (\%)$. Identities of skipped products were confirmed by sequencing.

Western Blot Analysis of Dystrophin Rescue

For protein extraction, 100 μL of a high SDS lysis buffer (10% SDS, 70 mM Tris-HCl [at pH 6.7], 5 mM EDTA at pH 8.0, 5% β -mercaptoethanol in water) with proteinase inhibitor cocktail (Roche) was added to 20- μm frozen muscle sections. This was mixed, incubated at 37°C for 5 min, and spun at max speed for 30 min at 16°C to collect the protein-containing supernatant. Protein was quantified using the Pierce Coomassie (Bradford) Protein Assay kit (Thermo Fisher). Protein was prepared by adding NuPAGE LDS Sample Buffer (Thermo Fisher) and NuPAGE Sample Reducing Agent (Thermo Fisher) at 1 \times final concentrations into the samples and then incubating at 70°C for 10 min. Western blotting was performed as described previously.⁴⁹ For non-treated and treated CXMD₁ dogs, 40 or 60 μg protein was used; 100%, 20%, 10%, or 5% of this was used for wild-type samples. The primary antibodies used, diluted using 2% Amersham ECL Prime blocking reagent (GE Healthcare) in PBS with 0.05% Tween 20 (PBST), were as follows: NCL-DYS1 (1:200, Leica Biosystems) for the dystrophin rod domain and desmin (1:4,000, Abcam) as a loading control. Appropriate horseradish peroxidase (HRP)-conjugated secondary antibodies (anti-mouse immunoglobulin G2a [IgG2a] for DYS1, anti-rabbit IgG H⁺L for desmin; Bio-Rad) were used at a 1:10,000 dilution in PBST. Post-transfer, the gel was stained with PageBlue Protein Staining Solution (Thermo Fisher) for 1 hr at room temperature to visualize myosin heavy chain (MyHC) as another loading control. Dystrophin levels were quantified from DYS1 band intensities, relative to the intensity of the wild-type band with 5% protein using ImageJ.

Immunohistochemistry

Frozen muscles from wild-type, non-treated CXMD₁, and treated CXMD₁ dogs were sectioned with 7- μm thickness and placed on poly-L-lysine-coated slides. Sections were air-dried for at least 30 min at room temperature. These were then incubated in NCL-DYS1 (1:50) or NCL-DYS2 (1:50, Leica Biosystems; targets the dystrophin C-terminal domain) and diluted in PBS with 0.1% Triton X-100 (PBSTX) for 1 hr at room temperature. Following three 5-min PBS washes, sections were incubated with Alexa Fluor 594-conjugated secondary antibodies (anti-mouse IgG2a for DYS1, anti-mouse IgG1 for DYS2; Thermo Fisher) at a 1:1,000 dilution in PBSTX for 1 hr at room temperature. After three 5-min PBS washes, samples were mounted with VECTASHIELD HardSet Antifade Mounting Medium with DAPI (Vector Laboratories). Samples were visualized in a blinded manner at a total magnification of 200 \times using the Zeiss LSM 710 confocal microscopy system or the Olympus FluoView laser-scanning microscope.

Histology

Samples were prepared as in the **Immunohistochemistry** section. Sections were stained using Mayer's H&E Y (Electron Microscopy

Sciences) following standard procedure. Samples were visualized at 200 \times magnification using a Nikon Eclipse TE2000-U microscope. Images were taken in at least three random fields of view per sample. Centrally nucleated fibers (CNFs) were quantified using ImageJ, with $([\# \text{ CNFs}]/[\text{total } \# \text{ fibers}]) \times 100 (\%)$. Around 200 to 2,800 of total myofibers were counted per muscle sample for CNF analysis. Fibrosis and/or necrosis was quantified following TREAT-NMD SOP DMD_M.1.2.007 v.1.0 and van Putten et al.⁵¹ ImageJ with the color deconvolution plugin (G. Landini, free from <http://www.mecourse.com/landing/software/cdeconv/cdeconv.html>) was used. The following was used for fibrosis and/or necrosis quantification: $([\text{fibrotic or necrotic area}]/[\text{total image area}]) \times 100 (\%)$. Values obtained across all fields of view were averaged for each sample. Image acquisition and both CNF and fibrosis and/or necrosis quantification were done blinded.

Blood Tests

Serum was obtained from weekly blood samples of treated CXMD₁ dogs and used for determining the levels of CK, BUN, CRE, AST, ALT, ALB, TBIL, GGT, TP, LDH, ALP, sodium (Na⁺), potassium (K⁺), and chloride (Cl⁻). These were also analyzed in sera from non-treated CXMD₁ and wild-type dogs at various ages to provide reference values. NCNP performed tests for all biomarkers, with additional tests by C-Path (Comparative Clinical Pathology Services, Columbia, MO) for ALB, ALP, and GGT.

ELISA

ELISA was performed based on the method by Burki et al.⁵² and in our previous study.⁴¹ PMOs in the blood were quantified using sera from weekly blood samples of treated CXMD₁ dogs or from age-matched samples of non-treated CXMD₁ and wild-type dogs. For PMO uptake quantification, protein was extracted from 20- μm frozen muscle sections using RIPA buffer (Thermo Fisher) with proteinase inhibitor cocktail (Roche). Lysates were incubated overnight at 55°C and then spun at maximum speed for 15 min to collect the protein-containing supernatant. Protein was quantified using the Pierce BCA Protein Assay kit (Thermo Fisher). Probes with complementary sequences to the PMOs used were synthesized (IDT) and modified at the 5' and 3' ends with digoxigenin and biotin, respectively; the first and last seven nucleotides were fully phosphorothioated.⁴¹ PMO amounts were calculated in reference to a standard curve constructed from fluorescence values given by the respective PMO standards.

Statistical Analysis

Statistical analysis was conducted using GraphPad Prism 7 (GraphPad Software). As appropriate, one-way ANOVA with Tukey's post-hoc test or Dunnett's multiple comparisons test, a one-tailed Student's t test or Welch t test was conducted to determine statistical significance.

SUPPLEMENTAL INFORMATION

Supplemental Information includes four figures and one table and can be found with this article online at <https://doi.org/10.1016/j.ymthe.2018.10.011>.

AUTHOR CONTRIBUTIONS

T.P., S.T., and T.Y. conceived and designed the study. Y.A., R.M., S.T., and T.Y. supervised the study. K.R.Q.L., Y.E., T.N., M. Kuraoka, M. Kobayashi, and T.Y. performed the experiments. T.N., M. Kuraoka, M. Kobayashi, and Y.A. managed the animals in the study. K.R.Q.L. and T.Y. wrote the manuscript.

CONFLICTS OF INTEREST

T.Y. received consulting fees from AGADA Biosciences. S.T. received consulting fees from Nippon Shinyaku, TAIHO PHARMA, and Daiichi-Sankyo; both are for work unrelated to this study.

ACKNOWLEDGMENTS

We would like to thank Quynh Nguyen and Dyanna Melo (University of Alberta) for their technical assistance and support in the study. We would like to thank our funding sources, namely the University of Alberta, the Women and Children's Health Research Institute Graduate Studentship award and Innovation Grant, The Friends of Garrett Cumming Research Fund, Muscular Dystrophy Canada, the HM Toupin Neurological Science Research Fund, the Canadian Institutes of Health Research China-Canada Joint Health Research Initiative 132574 and Foundation Grant 143251, the NIH, the Canada Foundation for Innovation Infrastructure Operating Fund 30819, Alberta Enterprise and Advanced Education, Jesse's Journey - Foundation for Gene and Cell Therapy, and Parent Project Muscular Dystrophy.

REFERENCES

- Mendell, J.R., Shilling, C., Leslie, N.D., Flanigan, K.M., al-Dahhak, R., Gastier-Foster, J., Kneile, K., Dunn, D.M., Duval, B., Aoyagi, A., et al. (2012). Evidence-based path to newborn screening for Duchenne muscular dystrophy. *Ann. Neurol.* *71*, 304–313.
- Bushby, K., Finkel, R., Birmkrant, D.J., Case, L.E., Clemens, P.R., Cripe, L., Kaul, A., Kinnett, K., McDonald, C., Pandya, S., et al.; DMD Care Considerations Working Group (2010). Diagnosis and management of Duchenne muscular dystrophy, part 1: diagnosis, and pharmacological and psychosocial management. *Lancet Neurol.* *9*, 77–93.
- Manzur, A.Y., Kinali, M., and Muntoni, F. (2008). Update on the management of Duchenne muscular dystrophy. *Arch. Dis. Child.* *93*, 986–990.
- van Deutekom, J.C.T., and van Ommen, G.-J.B. (2003). Advances in Duchenne muscular dystrophy gene therapy. *Nat. Rev. Genet.* *4*, 774–783.
- Ervasti, J.M. (2007). Dystrophin, its interactions with other proteins, and implications for muscular dystrophy. *Biochim. Biophys. Acta* *1772*, 108–117.
- Ervasti, J.M., and Campbell, K.P. (1993). A role for the dystrophin-glycoprotein complex as a transmembrane linker between laminin and actin. *J. Cell Biol.* *122*, 809–823.
- Mah, J.K. (2016). Current and emerging treatment strategies for Duchenne muscular dystrophy. *Neuropsychiatr. Dis. Treat.* *12*, 1795–1807.
- Monaco, A.P., Bertelson, C.J., Liechti-Gallati, S., Moser, H., and Kunkel, L.M. (1988). An explanation for the phenotypic differences between patients bearing partial deletions of the DMD locus. *Genomics* *2*, 90–95.
- Koenig, M., Beggs, A.H., Moyer, M., Scherpf, S., Heindrich, K., Bettecken, T., Meng, G., Müller, C.R., Lindlöf, M., Kaariainen, H., et al. (1989). The molecular basis for Duchenne versus Becker muscular dystrophy: correlation of severity with type of deletion. *Am. J. Hum. Genet.* *45*, 498–506.
- Mann, C.J., Honeyman, K., Cheng, A.J., Ly, T., Lloyd, F., Fletcher, S., Morgan, J.E., Partridge, T.A., and Wilton, S.D. (2001). Antisense-induced exon skipping and synthesis of dystrophin in the mdx mouse. *Proc. Natl. Acad. Sci. USA* *98*, 42–47.
- Gebski, B.L., Mann, C.J., Fletcher, S., and Wilton, S.D. (2003). Morpholino antisense oligonucleotide induced dystrophin exon 23 skipping in mdx mouse muscle. *Hum. Mol. Genet.* *12*, 1801–1811.
- Lu, Q.L., Mann, C.J., Lou, F., Bou-Gharios, G., Morris, G.E., Xue, S.A., Fletcher, S., Partridge, T.A., and Wilton, S.D. (2003). Functional amounts of dystrophin produced by skipping the mutated exon in the mdx dystrophic mouse. *Nat. Med.* *9*, 1009–1014.
- Lu, Q.L., Rabinowitz, A., Chen, Y.C., Yokota, T., Yin, H., Alter, J., Jadoon, A., Bou-Gharios, G., and Partridge, T. (2005). Systemic delivery of antisense oligonucleotide restores dystrophin expression in body-wide skeletal muscles. *Proc. Natl. Acad. Sci. USA* *102*, 198–203.
- Yokota, T., Lu, Q.L., Partridge, T., Kobayashi, M., Nakamura, A., Takeda, S., and Hoffman, E. (2009). Efficacy of systemic morpholino exon-skipping in Duchenne dystrophy dogs. *Ann. Neurol.* *65*, 667–676.
- Yokota, T., Duddy, W., and Partridge, T. (2007). Optimizing exon skipping therapies for DMD. *Acta Myol.* *26*, 179–184.
- Echigoya, Y., and Yokota, T. (2014). Skipping multiple exons of dystrophin transcripts using cocktail antisense oligonucleotides. *Nucleic Acid Ther.* *24*, 57–68.
- U.S. Food and Drug Administration (2016). FDA grants accelerated approval to first drug for Duchenne muscular dystrophy. <https://www.fda.gov/NewsEvents/Newsroom/PressAnnouncements/ucm521263.htm>.
- Lim, K.R.Q., Maruyama, R., and Yokota, T. (2017). Eteplirsin in the treatment of Duchenne muscular dystrophy. *Drug Des. Devel. Ther.* *11*, 533–545.
- Aartsma-Rus, A., and Krieg, A.M. (2017). FDA Approves Eteplirsin for Duchenne Muscular Dystrophy: The Next Chapter in the Eteplirsin Saga. *Nucleic Acid Ther.* *27*, 1–3.
- Sarepta Therapeutics (2017). Sarepta Therapeutics Announces Positive Results in Its Study Evaluating Gene Expression, Dystrophin Production, and Dystrophin Localization in Patients with Duchenne Muscular Dystrophy (DMD) Amenable to Skipping Exon 53 Treated with Golodirsin (SRP-4053). <https://globenewswire.com/news-release/2017/09/06/1108211/0/en/Sarepta-Therapeutics-Announces-Positive-Results-in-Its-Study-Evaluating-Gene-Expression-Dystrophin-Production-and-Dystrophin-Localization-in-Patients-with-Duchenne-Muscular-Dystrop.html>
- Aoki, Y., Nakamura, A., Yokota, T., Saito, T., Okazawa, H., Nagata, T., and Takeda, S. (2010). In-frame dystrophin following exon 51-skipping improves muscle pathology and function in the exon 52-deficient mdx mouse. *Mol. Ther.* *18*, 1995–2005.
- Merlini, L., Cicognani, A., Malaspina, E., Gennari, M., Gnudi, S., Talim, B., and Franzoni, E. (2003). Early prednisone treatment in Duchenne muscular dystrophy. *Muscle Nerve* *27*, 222–227.
- Merlini, L., Gennari, M., Malaspina, E., Ceconi, I., Armaroli, A., Gnudi, S., Talim, B., Ferlini, A., Cicognani, A., and Franzoni, E. (2012). Early corticosteroid treatment in 4 Duchenne muscular dystrophy patients: 14-year follow-up. *Muscle Nerve* *45*, 796–802.
- Raman, S.V., Hor, K.N., Mazur, W., Halnon, N.J., Kissel, J.T., He, X., Tran, T., Smart, S., McCarthy, B., Taylor, M.D., et al. (2015). Eplerenone for early cardiomyopathy in Duchenne muscular dystrophy: a randomised, double-blind, placebo-controlled trial. *Lancet Neurol.* *14*, 153–161.
- Rafael-Fortney, J.A., Chimanji, N.S., Schill, K.E., Martin, C.D., Murray, J.D., Ganguly, R., Stangland, J.E., Tran, T., Xu, Y., Canan, B.D., et al. (2011). Early treatment with lisinopril and spironolactone preserves cardiac and skeletal muscle in Duchenne muscular dystrophy mice. *Circulation* *124*, 582–588.
- Shimatsu, Y., Katagiri, K., Furuta, T., Nakura, M., Tanioka, Y., Yuasa, K., Tomohiro, M., Komegaya, J.N., Nonaka, I., and Takeda, S. (2003). Canine X-linked muscular dystrophy in Japan (CXMDJ). *Exp. Anim.* *52*, 93–97.
- Yu, X., Bao, B., Echigoya, Y., and Yokota, T. (2015). Dystrophin-deficient large animal models: translational research and exon skipping. *Am. J. Transl. Res.* *7*, 1314–1331.
- Saito, T., Nakamura, A., Aoki, Y., Yokota, T., Okada, T., Osawa, M., and Takeda, S. (2010). Antisense PMO found in dystrophic dog model was effective in cells from exon 7-deleted DMD patient. *PLoS ONE* *5*, e12239.
- Yokota, T., Nakamura, A., Nagata, T., Saito, T., Kobayashi, M., Aoki, Y., Echigoya, Y., Partridge, T., Hoffman, E.P., and Takeda, S. (2012). Extensive and prolonged restoration of dystrophin expression with vivo-morpholino-mediated multiple exon skipping in dystrophic dogs. *Nucleic Acid Ther.* *22*, 306–315.

30. Gazzoli, I., Pulyakhina, I., Verwey, N.E., Ariyurek, Y., Laros, J.F., 't Hoen, P.A., and Aartsma-Rus, A. (2016). Non-sequential and multi-step splicing of the dystrophin transcript. *RNA Biol.* *13*, 290–305.
31. Urasawa, N., Wada, M.R., Machida, N., Yuasa, K., Shimatsu, Y., Wakao, Y., Yuasa, S., Sano, T., Nonaka, I., Nakamura, A., and Takeda, S. (2008). Selective vacuolar degeneration in dystrophin-deficient canine Purkinje fibers despite preservation of dystrophin-associated proteins with overexpression of Dp71. *Circulation* *117*, 2437–2448.
32. Klingler, W., Jurkat-Rott, K., Lehmann-Horn, F., and Schleip, R. (2012). The role of fibrosis in Duchenne muscular dystrophy. *Acta Myol.* *31*, 184–195.
33. Vila, M.C., Klimek, M.B., Novak, J.S., Rayavarapu, S., Uaesoontrachoon, K., Boehler, J.F., Fiorillo, A.A., Hogarth, M.W., Zhang, A., Shaughnessy, C., et al. (2015). Elusive sources of variability of dystrophin rescue by exon skipping. *Skelet. Muscle* *5*, 44.
34. Nakamura, A., Kobayashi, M., Kuraoka, M., Yuasa, K., Yugeta, N., Okada, T., and Takeda, S. (2013). Initial pulmonary respiration causes massive diaphragm damage and hyper-CKemia in Duchenne muscular dystrophy dog. *Sci. Rep.* *3*, 2183.
35. LoMauro, A., D'Angelo, M.G., and Aliverti, A. (2015). Assessment and management of respiratory function in patients with Duchenne muscular dystrophy: current and emerging options. *Ther. Clin. Risk Manag.* *11*, 1475–1488.
36. van den Bergen, J.C., Wokke, B.H., Janson, A.A., van Duinen, S.G., Hulsker, M.A., Ginjaar, H.B., van Deutekom, J.C., Aartsma-Rus, A., Kan, H.E., and Verschuuren, J.J. (2014). Dystrophin levels and clinical severity in Becker muscular dystrophy patients. *J. Neurol. Neurosurg. Psychiatry* *85*, 747–753.
37. van Putten, M., Hulsker, M., Young, C., Nadarajah, V.D., Heemskerk, H., van der Weerd, L., 't Hoen, P.A., van Ommen, G.J., and Aartsma-Rus, A.M. (2013). Low dystrophin levels increase survival and improve muscle pathology and function in dystrophin/utrophin double-knockout mice. *FASEB J.* *27*, 2484–2495.
38. Yokota, T., Takeda, S., Lu, Q.L., Partridge, T.A., Nakamura, A., and Hoffman, E.P. (2009). A renaissance for antisense oligonucleotide drugs in neurology: exon skipping breaks new ground. *Arch. Neurol.* *66*, 32–38.
39. Aoki, Y., Nagata, T., Yokota, T., Nakamura, A., Wood, M.J., Partridge, T., and Takeda, S. (2013). Highly efficient in vivo delivery of PMO into regenerating myotubes and rescue in laminin- α 2 chain-null congenital muscular dystrophy mice. *Hum. Mol. Genet.* *22*, 4914–4928.
40. Novak, J.S., Hogarth, M.W., Boehler, J.F., Nearing, M., Vila, M.C., Heredia, R., Fiorillo, A.A., Zhang, A., Hathout, Y., Hoffman, E.P., et al. (2017). Myoblasts and macrophages are required for therapeutic morpholino antisense oligonucleotide delivery to dystrophic muscle. *Nat. Commun.* *8*, 941.
41. Echigoya, Y., Nakamura, A., Nagata, T., Urasawa, N., Lim, K.R.Q., Trieu, N., Panesar, D., Kuraoka, M., Moulton, H.M., Saito, T., et al. (2017). Effects of systemic multiexon skipping with peptide-conjugated morpholinos in the heart of a dog model of Duchenne muscular dystrophy. *Proc. Natl. Acad. Sci. USA* *114*, 4213–4218.
42. Moulton, H.M., and Moulton, J.D. (2010). Morpholinos and their peptide conjugates: therapeutic promise and challenge for Duchenne muscular dystrophy. *Biochim. Biophys. Acta* *1798*, 2296–2303.
43. Yugeta, N., Urasawa, N., Fujii, Y., Yoshimura, M., Yuasa, K., Wada, M.R., Nakura, M., Shimatsu, Y., Tomohiro, M., Takahashi, A., et al. (2006). Cardiac involvement in Beagle-based canine X-linked muscular dystrophy in Japan (CXMDJ): electrocardiographic, echocardiographic, and morphologic studies. *BMC Cardiovasc. Disord.* *6*, 47.
44. Juliano, R.L. (2016). The delivery of therapeutic oligonucleotides. *Nucleic Acids Res.* *44*, 6518–6548.
45. Lehto, T., Castillo Alvarez, A., Gauck, S., Gait, M.J., Coursindel, T., Wood, M.J., Lebleu, B., and Boisguerin, P. (2014). Cellular trafficking determines the exon skipping activity of Pip6a-PMO in mdx skeletal and cardiac muscle cells. *Nucleic Acids Res.* *42*, 3207–3217.
46. Youngblood, D.S., Hatlevig, S.A., Hassinger, J.N., Iversen, P.L., and Moulton, H.M. (2007). Stability of cell-penetrating peptide-morpholino oligomer conjugates in human serum and in cells. *Bioconjug. Chem.* *18*, 50–60.
47. Järver, P., Coursindel, T., Andaloussi, S.E., Godfrey, C., Wood, M.J., and Gait, M.J. (2012). Peptide-mediated Cell and In Vivo Delivery of Antisense Oligonucleotides and siRNA. *Mol. Ther. Nucleic Acids* *1*, e27.
48. Miskew Nichols, B., Aoki, Y., Kuraoka, M., Lee, J.J., Takeda, S., and Yokota, T. (2016). Multi-exon Skipping Using Cocktail Antisense Oligonucleotides in the Canine X-linked Muscular Dystrophy. *J. Vis. Exp.* *111*, e53776.
49. Maruyama, R., Echigoya, Y., Caluseriu, O., Aoki, Y., Takeda, S., and Yokota, T. (2017). Systemic Delivery of Morpholinos to Skip Multiple Exons in a Dog Model of Duchenne Muscular Dystrophy. *Methods Mol. Biol.* *1565*, 201–213.
50. Shimatsu, Y., Yoshimura, M., Yuasa, K., Urasawa, N., Tomohiro, M., Nakura, M., Tanigawa, M., Nakamura, A., and Takeda, S. (2005). Major clinical and histopathological characteristics of canine X-linked muscular dystrophy in Japan, CXMDJ. *Acta Myol.* *24*, 145–154.
51. van Putten, M., de Winter, C., van Roon-Mom, W., van Ommen, G.J., 't Hoen, P.A., and Aartsma-Rus, A. (2010). A 3 months mild functional test regime does not affect disease parameters in young mdx mice. *Neuromuscul. Disord.* *20*, 273–280.
52. Burki, U., Keane, J., Blain, A., O'Donovan, L., Gait, M.J., Laval, S.H., and Straub, V. (2015). Development and Application of an Ultrasensitive Hybridization-Based ELISA Method for the Determination of Peptide-Conjugated Phosphorodiamidate Morpholino Oligonucleotides. *Nucleic Acid Ther.* *25*, 275–284.

YMTHE, Volume 27

Supplemental Information

Efficacy of Multi-exon Skipping Treatment

in Duchenne Muscular Dystrophy Dog

Model Neonates

Kenji Rowel Q. Lim, Yusuke Echigoya, Tetsuya Nagata, Mutsuki Kuraoka, Masanori Kobayashi, Yoshitsugu Aoki, Terence Partridge, Rika Maruyama, Shin'ichi Takeda, and Toshifumi Yokota

Supplementary Figures and Table

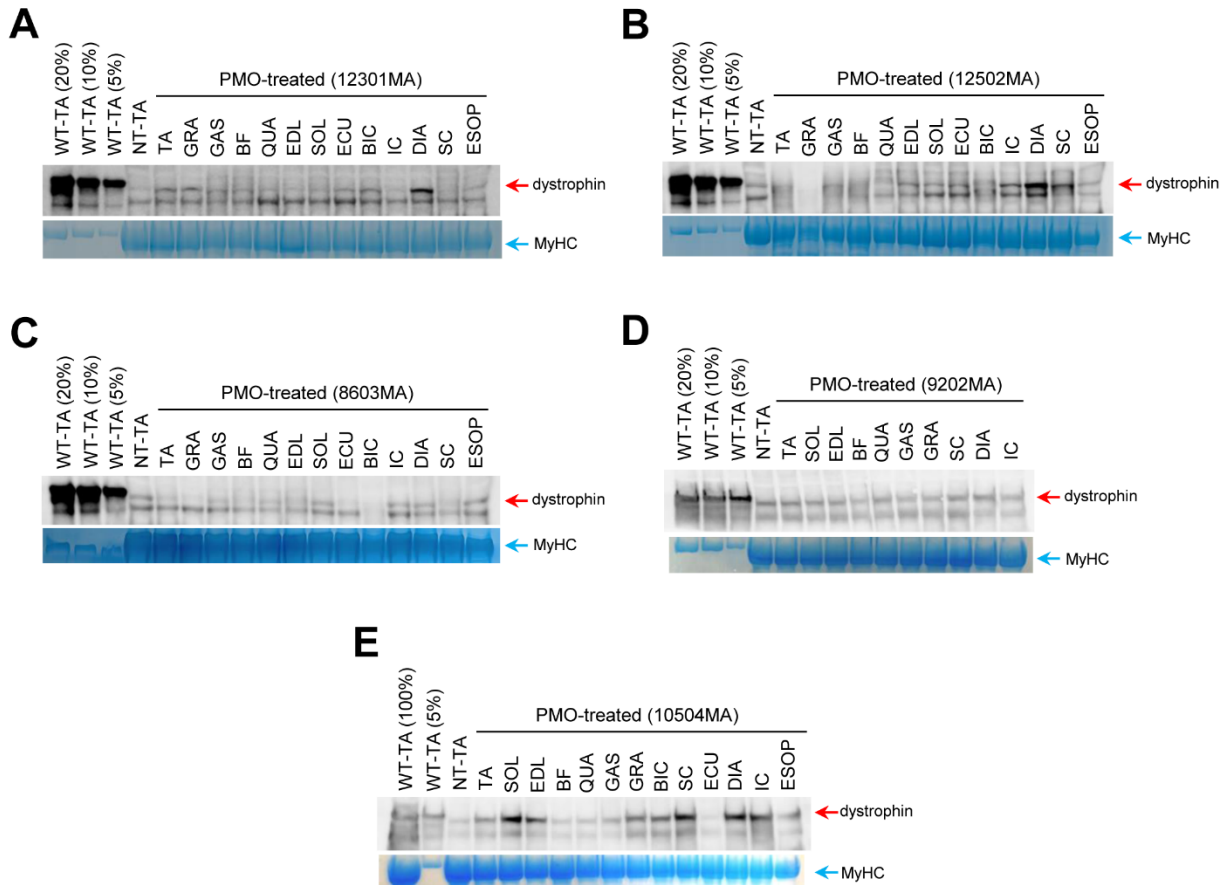


Figure S1. Dystrophin Western blot results for other treated CXMD_j neonatal dogs. Images showing dystrophin protein rescue in (A) 12301MA, (B) 12502MA, (C) 8603MA, (D) 9202MA, and (E) 10504MA. Myosin heavy chain (MyHC) is shown as a loading control. For (A) to (C), 40 μ g protein was loaded for non-treated (NT) and treated muscles; for (D) and (E), 60 μ g was loaded instead. Wild-type (WT) samples were loaded at the indicated levels, as percentages of the amounts loaded for the treated muscles. Abbreviations: TA, tibialis anterior; GRA, gracilis major; GAS, gastrocnemius; BF, biceps femoris; QUA, quadriceps; EDL, extensor digitorum longus; SOL, soleus; ECU, extensor carpi ulnaris; BIC, biceps brachii; IC, intercostal muscles; DIA, diaphragm; SC, sternocleidomastoid; ESOP, esophagus.

PMO-treated (8603MA)

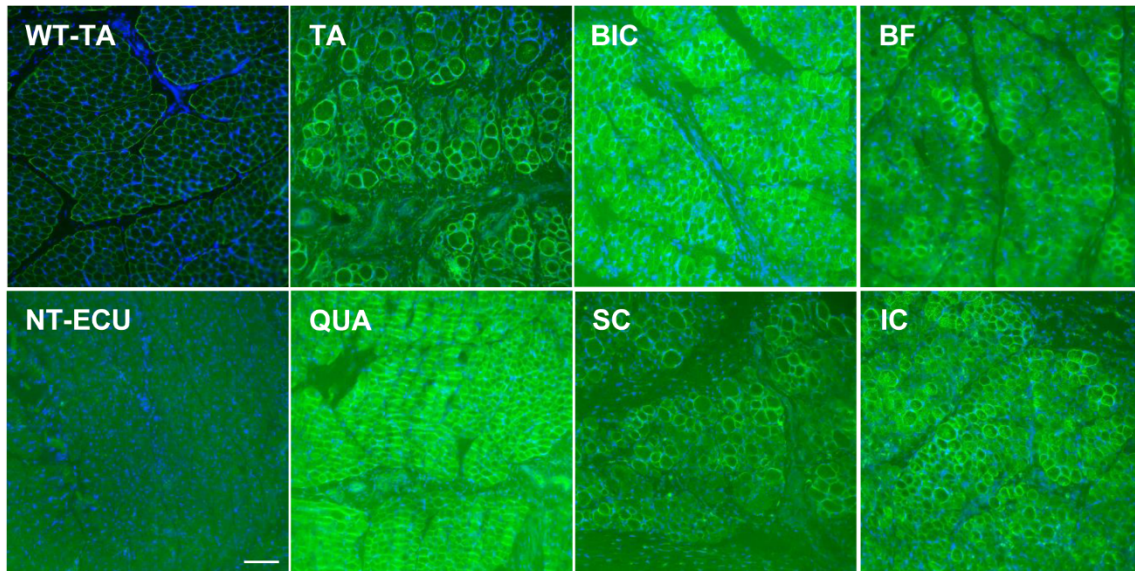


Figure S2. Representative immunohistochemistry images of skeletal muscles from 8603MA, stained using DYS1. Numerous dystrophin-positive fibers (green) can be observed in various skeletal muscles upon treatment; blue: nuclei. Total magnification: 200x; scale bar: 100 μ m. Abbreviations: TA, tibialis anterior; ECU, extensor carpi ulnaris; BIC, biceps brachii; BF, biceps femoris; QUA, quadriceps; SC, sternocleidomastoid; IC, intercostal muscles.

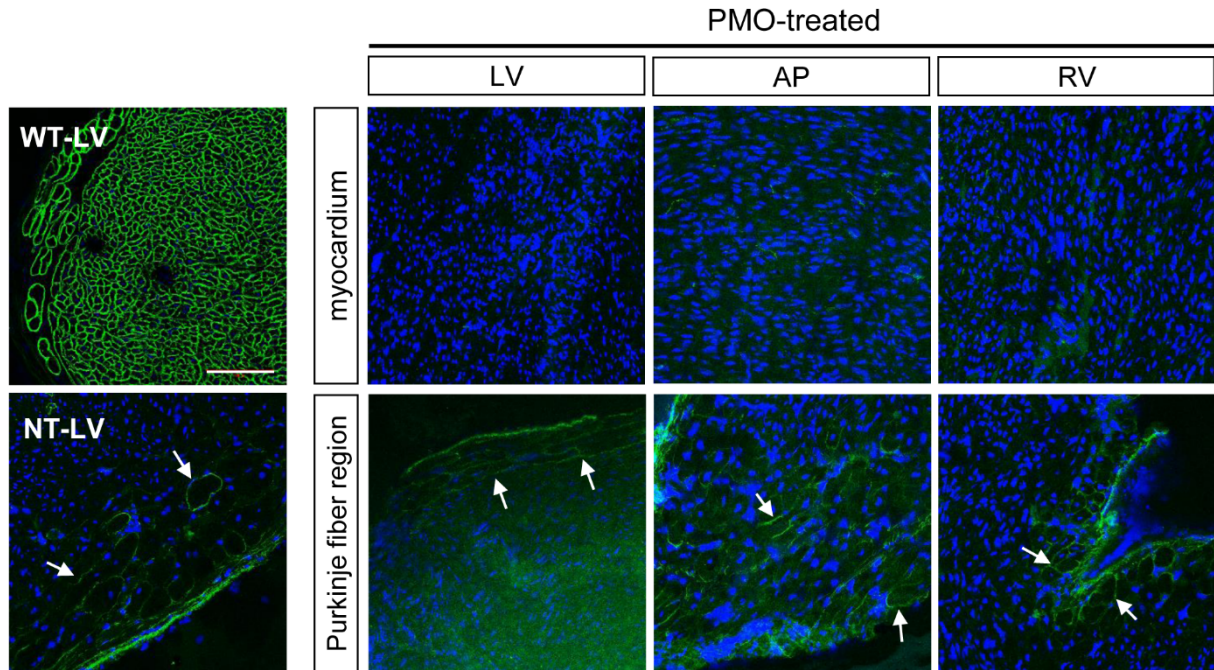


Figure S3. Representative immunohistochemistry images of cardiac muscles detected with DYS2. DYS2 is specific for the C-terminal domain of dystrophin. Dystrophin (green) can be detected in Purkinje fibers, as indicated by the white arrows, but not in the myocardium of treated CXMD_J dog cardiac muscles; blue: nuclei. Total magnification: 200x; scale bar: 100 μm. n = 4 (PMO-treated dogs). Abbreviations: WT, wild-type; NT, non-treated; LV, left ventricle; AP, anterior papillary muscle; RV, right ventricle.

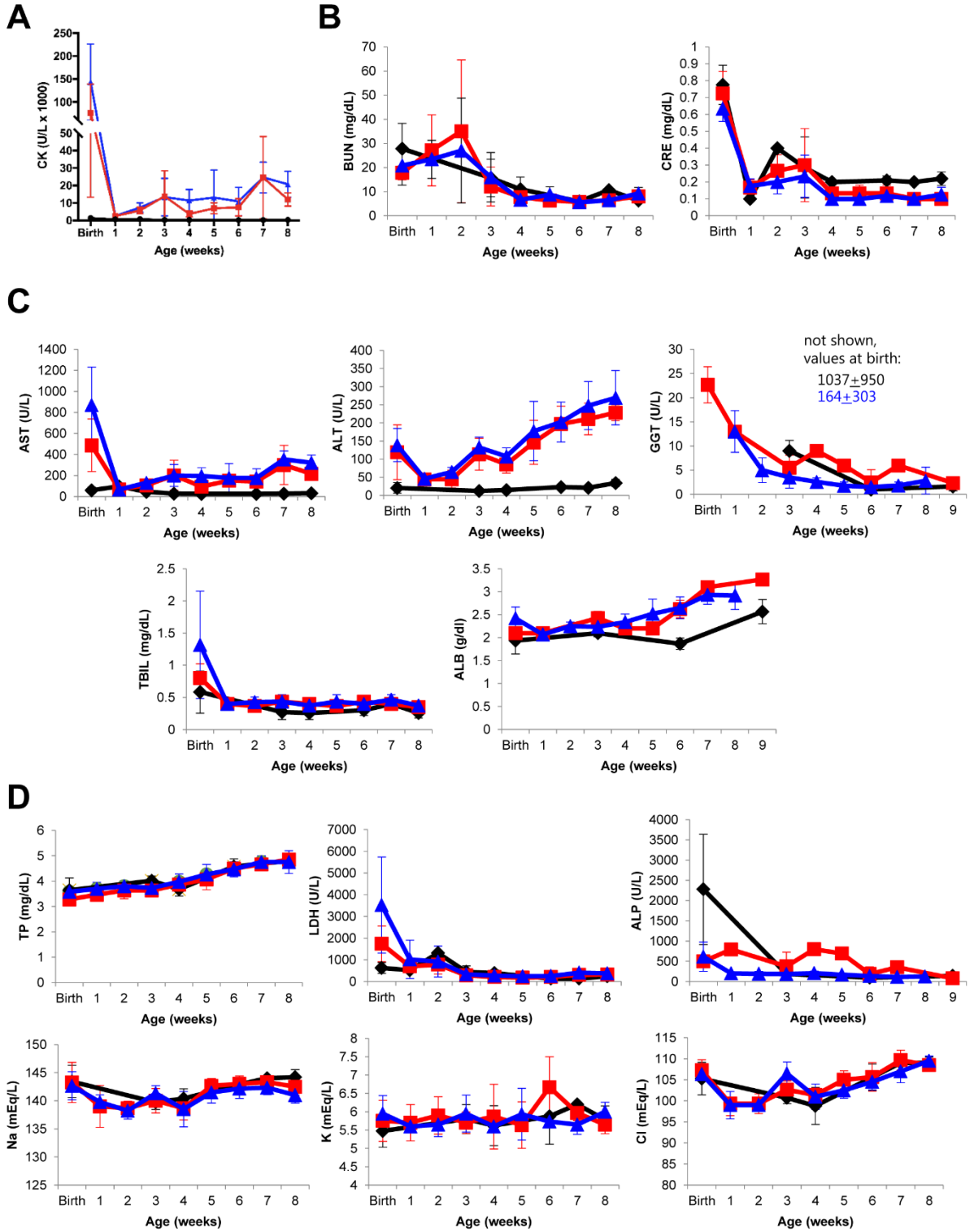


Figure S4. Analysis of serum biomarkers from weekly blood tests in neonatal dogs. The levels of various serum biomarkers were analyzed in weekly samples collected from wild-type

(black), non-treated CXMD₁ (red), and PMO-treated CXMD₁ (blue) dogs. (A) Creatine kinase (CK) levels. (B) Kidney damage marker levels: blood urea nitrogen (BUN), serum creatinine (CRE). (C) Liver damage marker levels: aspartate aminotransferase (AST), alanine aminotransferase (ALT), gamma-glutamyl transferase (GGT), total bilirubin (TBIL), serum albumin (ALB). (D) General marker levels: total protein (TP), lactate dehydrogenase (LDH), alkaline phosphatase (ALP), sodium (Na), potassium (K), chloride (Cl). Error bars: S.D. n = 1-12, wild-type; n = 3-4, non-treated; n = 4-6, treated.

Table S1. Comprehensive list of dogs used in the study.

Dog ID*	Treatment group	Functional testing				Molecular analyses**		Histology	ELISA (serum, tissues)	Blood tests
		Grading	15m run	Standing time	Open-mouth width	Skeletal muscles	Cardiac muscles			
8603MA	Treated		X			X	X	X	X	X
9202MA	Treated	X	X	X	X	X		X	X	X
10504MA	Treated	X	X	X	X	X		X	X	X
12301MA	Treated	X	X	X	X	X	X	X	X	X
12303MA	Treated	X	X	X	X	X	X	X	X	X
12502MA	Treated	X	X	X	X	X	X	X	X	X
8609MA	Non-treated		X					X		X
9201MA§	Non-treated									X
12305MA	Non-treated	X	X	X	X	X	X	X		X
12501MA	Non-treated	X	X	X	X	X	X	X		X
11403MA	Non-treated	X	X	X						
402MA	Non-treated					X		X		
2301MA	Non-treated							X		
3701MA	Non-treated			X	X					
5301FA	Non-treated			X	X					
5302FA	Non-treated			X	X					
5303MA	Non-treated			X	X					
5306MA	Non-treated			X	X					
5308FA	Non-treated			X	X					
8106MA	Non-treated			X	X					
11303MA	Non-treated			X	X					
14804MA	Non-treated									X
15001MA	Non-treated									X
15002MA	Non-treated									X
8601MN	Wild-type		X							X
9203MN	Wild-type		X	X	X					
10502MN	Wild-type	X	X	X	X	X	X	X		
12302MN	Wild-type	X	X	X	X	X		X		
12304MN	Wild-type					X		X		
12104MN	Wild-type	X	X	X						
601MN	Wild-type							X		
E09MN	Wild-type							X		
2303MN	Wild-type						X	X		
14003MN	Wild-type									X
14103MN	Wild-type									X
14104MN	Wild-type									X
14304MN	Wild-type									X
14402MN	Wild-type									X
14502MN	Wild-type									X
14504MN	Wild-type									X
14603MN	Wild-type									X
14701MN	Wild-type									X
14702MN	Wild-type									X
14703MN	Wild-type									X
14803MN	Wild-type									X

*the two letters at the end of each ID: the first indicates sex (M/F), the second indicates genotype (N = normal, A = affected, with CXMD_J mutation), **molecular analyses include: RT-PCR, Western blotting, immunohistochemistry, §died prior to endpoint.